Tribology Transactions

ISSN: 1040-2004 (Print) 1547-397X (Online) Journal homepage: https://www.tandfonline.com/loi/utrb20

Study on Static Supporting Capacity and Tribological Performance of Ferrofluids

WEI HUANG , CONG SHEN & XIAOLEI WANG

To cite this article: WEI HUANG , CONG SHEN & XIAOLEI WANG (2009) Study on Static Supporting Capacity and Tribological Performance of Ferrofluids, Tribology Transactions, 52:5, 717-723, DOI: 10.1080/10402000902913337

To link to this article: https://doi.org/10.1080/10402000902913337

Tribology Transactions, 52: 717-723, 2009

ISSN: 1040-2004 print / 1547-397X online
DOI: 10.1080/10402000902913337

STLE
Society of Tribologists
and Lubrication Engineers

Study on Static Supporting Capacity and Tribological Performance of Ferrofluids

WEI HUANG, CONG SHEN, and XIAOLEI WANG
College of Mechanical and Electrical Engineering
Nanjing University of Aeronautics & Astronautics
Nanjing 210016, P.R. China

In this article, Fe_3O_4-based ferrofluids (MFs) with different saturation magnetization (Ms) were prepared by the coprecipitation technique. The static supporting capacity of the different magnetization MF drops with a permanent magnet was tested using UMT-2 multi-specimen test system. The tribological performance of the carrier liquid and MF were conducted on a ring-on-cylinder tribometer. The results show that MF under a magnet has a higher supporting capacity compared with the carrier liquid and the supporting capacity of MF increases with the increase of Ms. With an external magnetic field applied, significant improvement in antifriction and wear resistance was obtained by using MF with proper Ms as lubricants.

KEY WORDS

Ferrofluids; Static Supporting Capacity; Sliding Friction; Wear; Viscosity

INTRODUCTION

Ferrofluids (MFs) are stable colloidal suspensions composed of single-domain magnetic nanoparticles dispersed in a carrier liquid (Shen, et al. *(1)*). The particles are usually made from magnetite (Fe_3O_4) and have a mean diameter of about 10 nm. Brownian motion keeps the magnetic particles from settling under gravity and the surfactant is placed around each particle to provide short-range steric repulsion between particles to prevent particle agglomeration. Many properties of the MF—e.g., vapor pressure, pour point, and chemical properties—are similar to those of the carrier liquid since the concentration of the magnetic particles is low. But there is an increase of the viscosity compared with the carrier liquid due to the existence of the nanoparticles. Stable suspensions of this kind were first synthesized in 1964 by Papell (see Odenbach *(2)*) and have since even reached technical importance in everyday life.

The behavior of MFs is mainly determined by their magnetic properties. Each particle can be treated as a thermally agitated permanent magnet in the carrier liquid (Odenbach *(2)*). The homogeneous fluids can be magnetized by applying an external magnetic field but still retain the properties of the fluid. These fluids show unusual properties; e.g., they can be confined, positioned, shaped, and controlled at desired places by applying an external magnetic field. This leads to important applications of MF lubrication in liquid seals, roller bearings, and journal bearings with small or nonexistent side leakage (Chandra, et al. *(3)*; Miyake and Takahashi *(4)*). Up to now, most reports on MF lubrication have focused on theoretical studies (Nada and Osman *(5)*; Osman, et al. *(6)*; Sinha, et al. *(7)*; Shan and Bhat *(8)*) and few have been seen in experimental studies.

In this article, Fe_3O_4-based MFs with different saturation magnetization (Ms) were prepared by the coprecipitation technique. The purpose of this research is to investigate the static supporting capacity and the tribological properties of MFs under an external magnetic field. The static supporting capacity of the Fe_3O_4-based MFs with different Ms under an external magnetic field was tested. Compared with the carrier liquid, the tribological properties of the MFs in the presence of an external magnetic field were investigated by a ring-on-cylinder tribometer.

EXPERIMENTAL DETAILS

First, the Fe_3O_4 nanoparticles coated with a primary surfactant (oleic acid) were obtained by the coprecipitation technique. The water in the particles was removed by washing with acetone. The resulting particles coated with a secondary surfactant (succinicimide) were dispersed in α-olefinic hydrocarbon synthetic oil (PAO4) by ultrasonic. The final fluid was centrifuged at 12,000 rpm for 10 min and the detailed synthetic procedures can be found elsewhere (Sutariya, et al. *(9)*). TEM image (Fig. 1) shows that the Fe_3O_4 nanoparticles are nearly spherical and the average size is 14 ± 2 nm. The Ms of the MF samples was examined by an LDJ9600 Vibrating Sample Magnetometer (VSM). The stability of the MFs prepared was roughly estimated from the particle suspending percentage (Huang and Wang *(10)*). After resting for 10 days, the particle suspension percentage of all the MF samples remained above 98%. This means that the magnetic particles are coated completely by the surfactant and dispersed in the carrier liquid homogeneously. The volume fraction (vol%) of the particles in the MF was calculated according to Huang, et al. *(10)*. The properties of the carrier liquid and MFs are given in Table 1.

Manuscript received November 5, 2008
Manuscript accepted March 15, 2009
Review led by Tom Karis

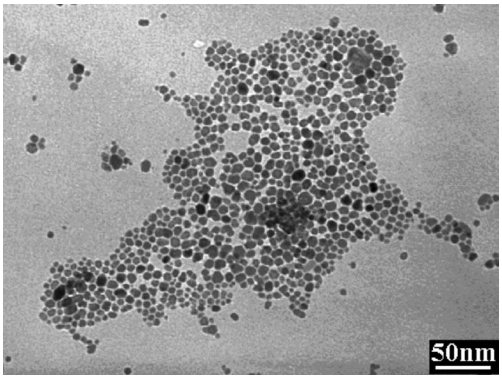

Fig. 1—TEM image of Fe_3O_4 particles.

The static supporting capacity of the MFs with a permanent magnet was performed using a UMT-2 multi-specimen test system that can measure the bearing force of the indenter automatically by a force sensor with its own offset variable. The cylinder (Fig. 2(a)) keeps resting and the plate (Fig. 2(b)) moves down. The supporting force of the MFs depends on the distance between the cylinder and the plate. Both the cylinder and the plate were made of aluminum (nonmagnetic metal) and the roughness of the end faces was 0.15 μm. There were 8 holes (φ 4.0 mm $\times$ 4.2 mm) in the cylinder and columniform NdFeB permanent magnets (φ 4.0 mm $\times$ 4.0 mm, magnetic property: 35 MGOe) were situated in every hole. All the magnets were put in the same magnetic pole direction. The distance between the two end surfaces (aluminum and NdFeB) is 0.2 mm. Figure 3 shows the surface magnetic field intensity distribution of the cylinder (Fig. 2(a)), which was calculated by Ansoft Designer 2.2 software. The theoretical basis of the calculation is Maxwell equations. The magnetic field strength (H) of the permanent magnet in a direction aligned with the poles was also calculated. The magnets are covered by drops of MF (1 mL) and it can be seen that small protrusions appear on the surface of the fluid (Fig. 2(c)). Before every test, the force sensor was zeroed. The supporting force of MF was recorded by a force sensor during the plate moving down. The moving distance was given by the UMT-2 multi-specimen test system. Since the cylinder and the plate were made of a nonmagnetic substance, the effect of the magnetic field was neglected. During the supporting force tests, gravity and the surface tension were also ignored.

The friction and wear tests lubricated with the carrier liquid and MFs were conducted on a ring-on-cylinder tribometer. Figure 4 shows the schematic diagram of the tribotester. The ring (Fig. 2(f)) is fixed on the rolling shaft driven by a motor with an adjustable rotational speed. The cylinder (Fig. 2(c)) is supported by a hemispherical tip so that its friction surface is automatically aligned to match the surface of the ring. The load is applied by a spring system from the bottom of the cylinder. The test conditions are listed in Table 2. The dosage of MF and carrier liquid used in experiments was also 1 mL.

TABLE 1—PROPERTIES OF CARRIER LIQUID AND MFS AT 20°C

Lubrication	Density (Kg/m^3)	Viscosity (mPa·s)	Ms (kA/m)	Volume Fraction of Particles (Vol%)
Carrier liquid (PAO4)	0.84×10^3	50	0	0
MF-1	1.05×10^3	67	15.9	4.83
MF-2	1.12×10^3	78	23.9	6.32
MF-3	1.21×10^3	95	31.8	8.52

RESULTS AND DISCUSSION

Supporting Capacity of the MF in the Presence of a Magnetic Field

Figure 5 shows that the static supporting force of MFs increases with the shifting down of the plate. After moving about 3.6 mm, the MF was extruded out when the plate and the cylinder contacted each other. The maximum supporting capacity of all the samples is at the inflexion of the curve. For the carrier liquid, there is no magnetic particle in it and the thickness of the oil film is about 1 mm. After moving down about 2.5 mm, the plate can just contact the carrier liquid on the cylinder.

In the presence of an external magnetic field, the single domain magnetic particles suspended in the carrier liquid become magnetized. Owing to the dipolar-dipolar interaction, a particle tends to attract the neighboring particles in the direction of its magnetic moment. This kind of attractive magnetic force shows itself as a body force on the liquid (Oldenburg, et al. *(11)*). For the nonconductive MF, the unit volume value of the induced magnetic force under the effect of the magnetic field can be written as (Nada and Osman *(5)*):

$$F_m = \mu_0 M_g \nabla H \qquad [1]$$

where μ_0 is the magnetic permeability of the free space, M_g is the magnetization of MF, and ∇H represents the gradient of the magnetic field.

In general, the magnetization (M_g) of the magnetic material is a function of temperature and the applied magnetic field. Considering the isothermal condition and linear behavior of the MF, Eq. [1] can be rewritten as (Osman, et al. *(6)*):

$$F_m = \mu_0 X_m h_m \nabla H \qquad [2]$$

where X_m is susceptibility of the ferrofluid; h_m is the magnetic field intensity.

The supporting force of the MFs is low at the beginning, which is caused by the little gradient of the magnetic field (see figure inset in Fig. 5). When the plate moves down about 2.5 mm, the supporting force of MF increases obviously. And at this position, the gradient of the magnetic field has an obvious increase also. According to Eq. [2], for the magnetization of MF-3>MF-2>MF-1, the supporting force is MF-3>MF-2>MF-1 when the plate is at the same position. Many theoretical and experimental studies have shown that the increase of the MF magnetization brings about a significant increase of the MF viscosity caused by particle interactions and polydispersivity (Iusan, et al. *(12)*). It is known that the increase of the viscosity will also enhance the supporting capacity of MF. Under the external field, the yield strength

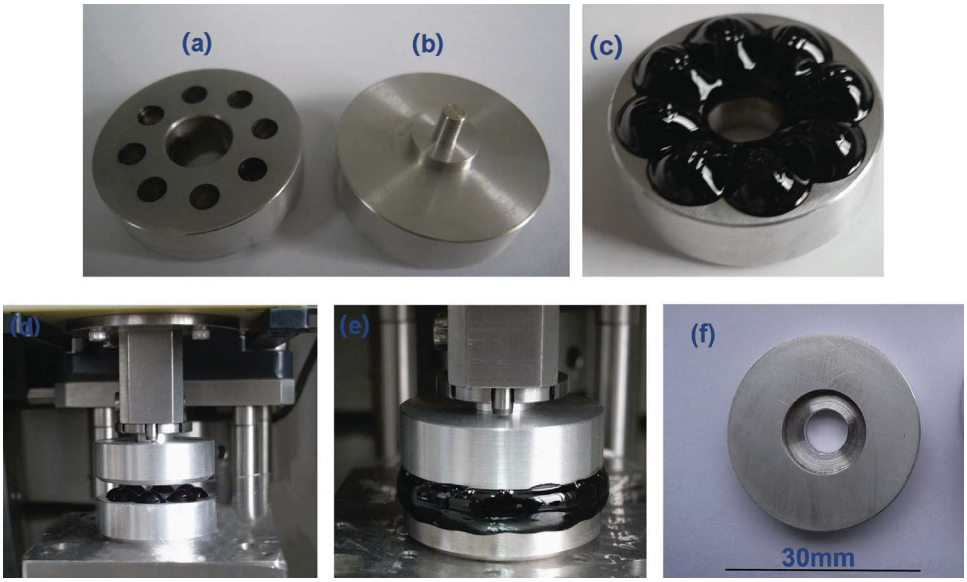

Fig. 2—Cylinder with magnets; (b) plate; (c) cylinder covered with magnetic fluid; (d) a photograph of test samples installed in the UMT-2; (e) a photograph of plate squeezing process; (f) ring as shown in Fig. 4.

of the MF will increase with the particle content. And as a result, the supporting capacity of MF will increase with increasing yield strength. When the plate moves over 3 mm, the static supporting capacity of the three MF samples steeply increases. It is mainly caused by two reasons: (a) a sudden increase of the magnetic gradient; (b) an increasing magnetization of the MF. The inset in Fig. 5 shows the calculated values of the magnetic field strength (H) in a direction aligned with the poles. It can be seen that for distances from the magnet less than 2 mm, the strength of the magnetic field changes quickly. This means that the closer to the magnet, the higher the magnetic field gradient and the magnetic field strength are. Since the magnetization of the MF is linear with the external magnetic field, the closer to the magnet, the higher the magnetization of the MF is. Referring to Eq. [2], it can be realized that the supporting force of MF is proportional to the product of the magnetization and the gradient of the field strength, which are both affected by the distance from the magnet. The differences of the supporting forces between different MFs are distinct when the distance between the plate and the cylinder is within 1 mm. When the plate moves down over

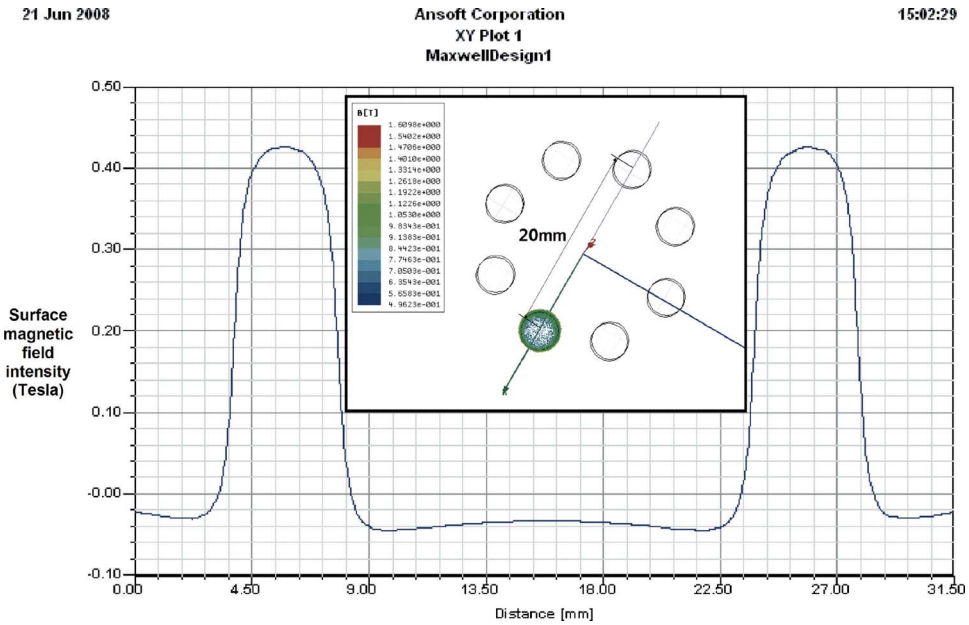

Fig. 3—Surface magnetic field intensity of cylinder (the inset shows the distribution of the eight permanent magnets).

TABLE 2—EXPERIMENTAL CONDITIONS

Normal pressures	0.04-0.20 MPa
Sliding velocities	0.052-0.364 m/s
Lubricant	Carrier liquid and magnetic fluids (see Table 1)

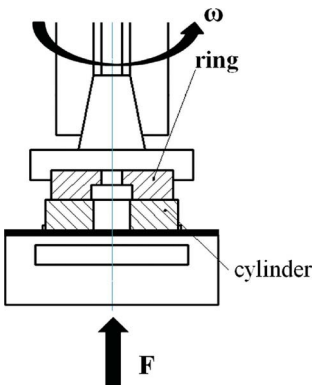

Fig. 4—Schematic diagram of tribotester.

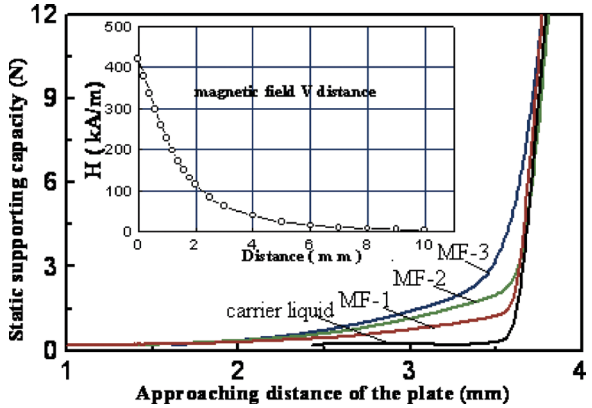

Fig. 5—Dependence of the supporting capacity on the distance between the cylinder and the plate (the inset shows the calculated values of the magnetic field strength (*H*) in the direction aligned with the poles).

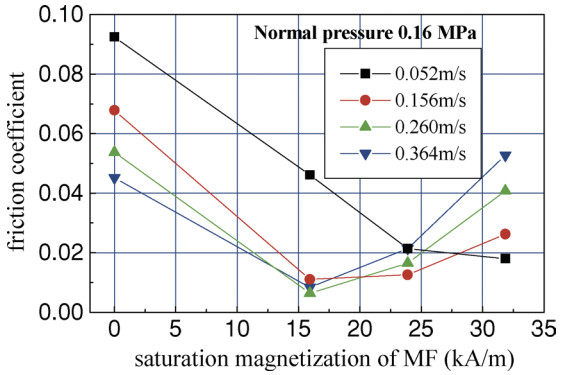

Fig. 6—The effect of different MFs on the friction coefficient with different sliding velocities.

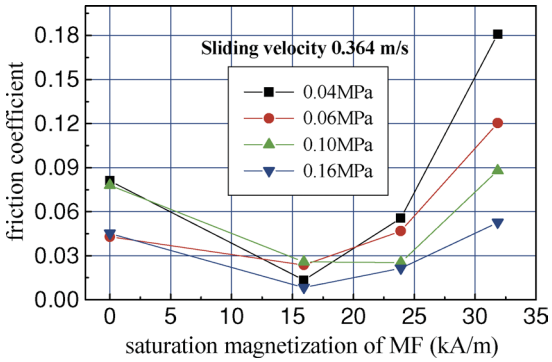

Fig. 7—The effect of different MFs on the friction coefficient with different normal pressures.

3.6 mm, the force increases linearly, which is caused by the distortion of aluminum.

Friction and Wear Tests Lubricated with Carrier Liquid and MF

Figure 6 shows the effects of the lubricants on the friction coefficient at the sliding velocities of 0.052, 0.156, 0.260, and 0.364 m/s, respectively. The normal pressure is fixed at 0.16 MPa. The lubricants are the carrier liquid and the MFs as shown in Table 1. When lubricated with the carrier liquid, the friction coefficients decrease with the sliding velocities. The high friction coefficients (0.092-0.045) suggest that it is in the state of mixed lubrication and that mechanical contact occurs between the sliding surfaces under these conditions. When lubricated with MF, the viscosity of MF increases significantly by the external magnetic field applied (Chikazumi, et al. *(13)*). The existence of the surfactant will also increase the viscosity of MF compared with the carrier. And as a result, the load-carrying capacity of the oil film will increase. When using 15.9 kA/m MF, at high sliding velocities (0.156, 0.260, and 0.364 m/s), the friction coefficients are in the range of 0.006-0.01, which is usually the friction coefficient of the full-film lubrication regime. It is known that the sliding velocity and the viscosity of the lubricants both have important effects on the friction coefficients according to the typical Stribeck curve

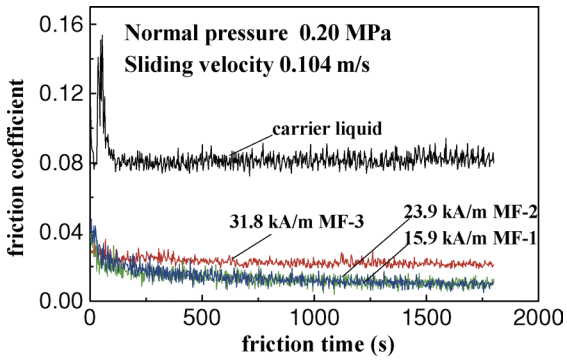

Fig. 8—Variation of the friction coefficient during the test carried out with different lubricants.

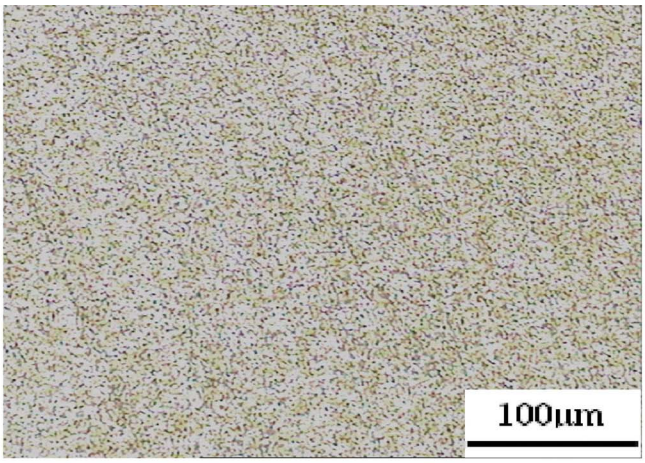

(a)

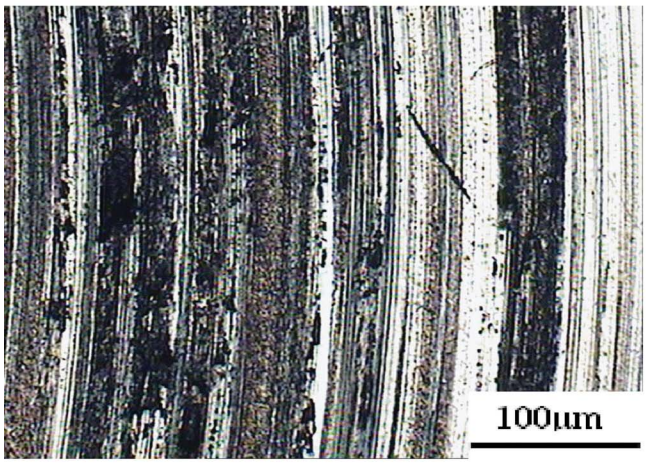

(b)

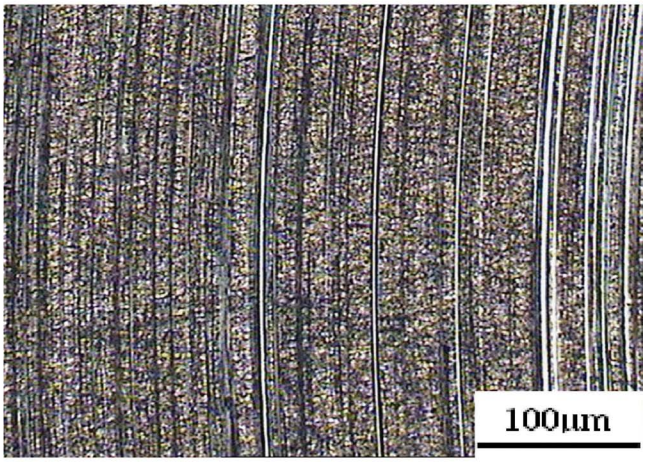

(c)

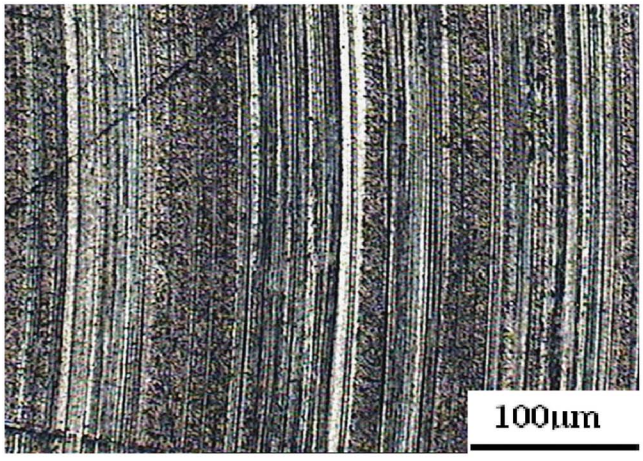

(d)

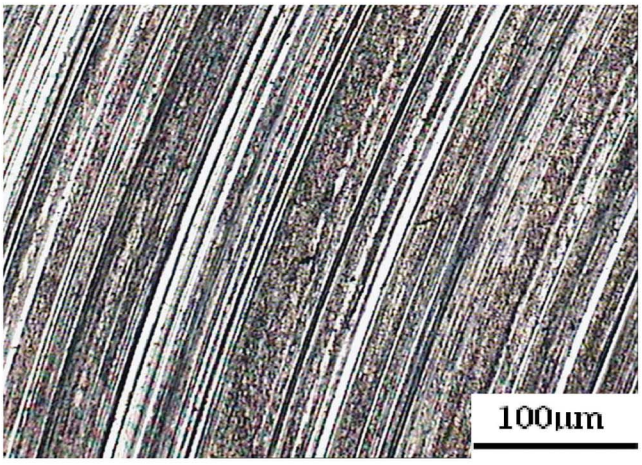

(e)

Fig. 9—Optical microscope images of a worn scar lubricated with carrier liquid and MFs. (a) Before test; (b) lubricated with carrier liquid; (c) lubricated with 15.9 kA/m MF; (d) lubricated with 23.9 kA/m MF; (e) lubricated with 31.8 kA/m MF.

TABLE 3—SURFACE ROUGHNESS AND MASS OF THE FIXED RINGS BEFORE AND AFTER TEST

	Lubricants							
	Carrier Liquid		15.9 kA/m MF-1		23.9 kA/m MF-2		31.8 kA/m MF-3	
	Before	After	Before	After	Before	After	Before	After
Ra (μm)	0.15	0.49	0.15	0.20	0.15	0.24	0.15	0.33
ΔRa (μm)	0.34		0.05		0.09		0.18	
m (g)	7.2666	7.2609	7.3490	7.3479	7.1914	7.1904	7.2571	7.2557
Δm (g)	0.0057		0.0011		0.0010		0.0014	

(Wen and Huang *(14)*). The nanoparticles in the carrier liquid may produce the the ball effects between the frictional couples (Huang, et al. *(15)*). At low particle content, the nanoparticles may move freely, which can improve the tribological properties of MF-1. When 23.9 kA/m and 31.8 kA/m MF are used, their viscosity will increase significantly in the presence of the external magnetic field and the oil film will become thicker, which leads to an increase in the friction coefficients. Another explanation is that some coagulation has formed due to the ferromagnetism of the particles, though the shear may decrease the coagulation of the particles. This kind of coagulation in high-concentration MF would reduce the ball effect.

Figure 7 shows the effects of the lubricants on the friction coefficient at a normal pressure of 0.04, 0.06, 0.10, and 0.16 MPa, respectively. The sliding velocity is fixed at 0.364 m/s. Compared with the carrier liquid, the four friction coefficients lubricated with 15.9 kA/m MF decrease obviously. In the presence of a magnet, MF can be partially retained on the interface and the proper increase of the viscosity of the 15.9 kA/m MF under the external magnetic field may decrease the friction coefficients. It can be seen that the friction coefficients increase with the increase of magnetization of the MF. As mentioned above, the increase of friction coefficients is mainly caused by the increase of MF viscosity. The friction coefficients lubricated with 31.8 kA/m MF increase with decreasing loads, which is also coincidental with the Stribeck curve.

Figure 8 shows the friction properties lubricated with the carrier liquid and the MFs, respectively. The optical microscope (OM) images of the worn surface are shown in Fig. 9. As can be seen in Fig. 8, the friction coefficient of the carrier liquid is much higher than that of the MFs. And the friction coefficient is approximately 0.08, which is in the mixed-film lubrication regime. The friction coefficient lubricated with 31.8 kA/m MF is a little higher than that of the 15.9 and 23.9 kA/m MF, which may be caused by the increase of the MF viscosity.

Figure 9(a) shows the ring surface before the test. It can be found that the worn surface lubricated by the carrier liquid shown in Fig. 9(b) is evidently rough, with many thick and deep furrows but the rubbing surface lubricated by the MF is rather smooth and the furrows are rather shallow (Figs. 9(c), 9(d), and 9(e)). It shows that MF has good friction-reduction behavior under an external magnetic field. The heterogeneous wear scars (Fig. 9(d) and 9(e)) may be caused by some particle coagulation for the high concentration of MF-2 and MF-3.

The arithmetic mean value of the surface roughness (Ra) and the difference in roughness before and after the test of the fixed rings are shown in Table 3, and the difference in mass before and after the test of the fixed rings is also shown in this table. The smaller ΔRa and Δm indicate better tribological performance between the contact specimens. As can be seen in Table 3, the ΔRa and Δm of the 15.9 and 23.9 kA/m MFs are much smaller than that of the carrier liquid and 31.8 kA/m MF. This result is in accordance with the best friction-reduction performance of 15.9 and 23.9 kA/m MFs as shown in Fig. 6 and Fig. 7.

CONCLUSIONS

Under an external magnetic field, the static supporting capacity and the tribological behavior of the MF were examined compared with the carrier liquid. The results show that the supporting capacity of MF increases with the increase of saturation magnetization. There is a sudden increase of the supporting capacity when the MF thickness is less than 1 mm. And it is caused by the increase of the gradient of field strength. The friction results indicate that 15.9 kA/m MF has good friction-reduction behavior in the presence of an external magnetic field (magnetic property: 35 MGOe). The supporting capacity and the tribological behavior of the MFs with different magnets will be examined in further work.

ACKNOWLEDGEMENT

This work was supported by the National Natural Science Foundation of China (No. 50875125).

REFERENCES

(1) Shen, L., Laibinis, P. E. and Hatton, T. A. (1999), "Aqueous Magnetic Fluids Stabilized by Surfactant Bilayers," *J. Magn. Magn. Mater.*, **194**, pp 37-44.

(2) Odenbach, S. (2003), "Magnetic Fluids-Suspensions of Magnetic Dipoles and their Magnetic Control," *J. Phys.: Condens. Matter*, **15**, pp S1497-S1508.

(3) Chandra, P., Sinha, P. and Kumar, D. (1992), "Ferrofluid Lubrication of a Journal Bearing Considering Cavitation," *Tribol. Trans.*, **35**(1), pp 163-169.

(4) Miyake, S. and Takahashi, S. (1985), "Sliding Bearing Lubrication with Ferromagnetic Fluid," *Tribol. Trans.*, **28**(4), pp 461-466.

(5) Nada, G. S. and Osman, T. A. (2007), "Static Performance of Finite Hydrodynamic Journal Bearings Lubricated by Magnetic Fluids with Couple Stesses," *Tribol. Lett.*, **27**, pp 261-268.

(6) Osman, T. A., Nada, G. S. and Safar, Z. S. (2003), "Different Magnetic Models in the Design of Hydrodynamic Journal Bearings Lubricated with Non-Newtonian Ferrofluid," *Tribol. Lett.*, **14**, pp 211-223.

(7) Sinha, P., Kanpur, P. C. and Kumar, D. (1993), "Ferrofluid Lubrication of Cylindrical Rollers with Aavitation," *Acta Mechanica*, **98**, pp 27-38.

(8) Shan, R. C. and Bhat, M.V. (2005), "Ferrofluid Squeeze Film between Curved Annular Plates Including Rotation of Magnetic Particles," *J. Eng. Mathe.*, **51**, pp 317-324.

(9) Sutariya, G. M., Upadhyay, R. V. and Mehta, R.V. (1993), "Preparation and Properties of Stable Magnetic Fluid Using Mn Substituted Ferrite Particles," *J. Colloid Interface Sci.*, **155**, pp 152-155.

(10) Huang, W. and Wang, X. L. (2008), "Preparation and Properties of ε-Fe_3N Based Magnetic Fluid," *Nanoscale Res. Lett*., **3**, pp 260-264.

(11) Oldenburg, C. M., Borglin, S. E. and Moridis, G. J. (2000), "Numerical Simulation of Ferrofluid Flow for Subsurface Environmental Engineering Applications," *Transport in Porous Media,* **38**, pp 319-344.

(12) Iusan, V., Bioca, C. D. and Hadgia, S. (1999), "Mangetic Fluids of Low Viscosity," *J. Magn. Magn. Mater.*, **201**, pp 38-40.

(13) Chikazumi, S., Taketomi, S., Ukita, M., Mizukami, M., Miyajima, H., Setogawa, M. and Kurihara, Y. (1987), "Physics of Magnetic Fluids," *J. Magn. Magn. Mater.*, **65**, pp 245-251.

(14) Wen, S. and Huang, P. (2002), *The Principle of Tribology*, 2nd Ed., Tsinghua Press, Beijing, P.R. China.

(15) Huang, H. D., Tu, J. P., Gan, L. P. and Li, C. Z. (2006), "An Investigation on Tribological Properties of Graphite Nanosheets as Oil Additive," *Wear,* **261**, pp 140-144.